MVA-ST Vaccination in an Aged-Hamster Model for COVID-19 Overcomes Age-Related Immune Dysfunction and Robustly Activates T Cells and Antibodies

Sabrina Clever , Lisa-Marie Schünemann , Federico Armando , Christian Meyer zu Natrup , Tamara Tuchel , Alina Tscherne , Malgorzata Ciurkiewicz , Wolfgang Baumgärtner , Gerd Sutter Sutter , Asisa Volz *

Posted Date: 29 November 2023

doi: 10.20944/preprints202311.1882.v1

Keywords: poxvirus; recombinant vaccine; preclinical model; vaccination elderly

Article

MVA-ST Vaccination in an Aged-Hamster Model for COVID-19 Overcomes Age-Related Immune Dysfunction and Robustly Activates T Cells and Antibodies

Sabrina Clever [1], Lisa-Marie Schünemann [1], Federico Armando [2,3], Christian Meyer zu Natrup [1], Tamara Tuchel [1], Alina Tscherne [3], Malgorzata Ciurkiewicz [2], Wolfgang Baumgärtner [2], Gerd Sutter [3] and Asisa Volz [1,*]

[1] Institute of Virology, University of Veterinary Medicine Hannover, Buenteweg 17, 30559 Hanover, Germany
[2] Department of Pathology, University of Veterinary Medicine Hannover, Buenteweg 17, 30559 Hanover, Germany
[3] University of Parma, Department of Veterinary Science, Pathology Unit, Parma, Italy
* Correspondence: Asisa.Volz@tiho-hannover.de; Tel.: +49 511 953-8857

Abstract: Aging is associated with a decline in immune system functionality. So-called immunosenescence may impair successful vaccination of elderly people. Thus, improved vaccination strategies specifically adapted to an aged immune system are required. We characterized a recombinant MVA expressing a stabilized version of SARS-CoV-2 S protein (MVA-ST) in an aged-hamster model for COVID-19. Intramuscular MVA-ST immunization resulted in protection from disease and severe lung pathology. Importantly, protection correlated with potent activation of SARS-CoV-2 specific T-cells and neutralizing antibodies. Our results suggest that MVA vector vaccines merit further evaluation as clinical candidate vaccines in elderly people to overcome limitations of age-dependent immunosenescence.

Keywords: poxvirus; recombinant vaccine; preclinical model; vaccination elderly

1. Introduction

SARS-CoV-2 infection in elderly people has been demonstrated to result in more severe morbidity and mortality [1]. In addition, the efficacy of COVID-19 vaccines against symptomatic infection was lower in older adults (age ≥60 years) compared with younger individuals [2] confirming previous data from the evaluation of Flu vaccines in elderly [3].

The Syrian hamster model has been established as a surrogate model for COVID-19 in humans. Previous studies confirmed that SARS-CoV-2 infection of aged hamsters (28-40 week old), as opposed to 6-8 week-old adults, resulted in more severe disease outcomes, mimicking the disease phenotype seen in elderly humans [4–6].

Modified Vaccinia virus Ankara (MVA), a safety-tested and replication-deficient vaccinia virus, is licensed as a third-generation smallpox vaccine. In addition, MVA also serves as an advanced vaccine technology platform for developing viral vector vaccines against infectious diseases and cancer. Moreover, MVA is part of a licensed heterologous prime-boost vector vaccine against Ebola virus (EBOV) in combination with a recombinant adenovirus vector [7–9].

Previously, we confirmed that an MVA-based candidate vaccine against COVID-19 expressing a prefusion stabilized SARS-CoV-2 spike protein (MVA-ST) was safe, immunogenic and effective when tested in k18-hACE2 mice (6-8 week old) and hamsters (10 week old) [10]. These results demonstrated safety, immunogenicity and protective outcome in adult animals. Moreover, the safety and robust activation of specific immune responses of this MVA-ST candidate vaccine have been confirmed in phase I clinical testing in humans (unpublished data). Here, we set out to evaluate the

 doi:10.20944/preprints202311.1882.v1

safety, immunogenicity and efficacy of MVA-ST vaccination in aged hamsters. Prime-boost intramuscular MVA-ST immunization sufficiently prevented severe disease outcomes in aged hamsters. This protective capacity correlated with robust activation of neutralizing antibodies and T cells in MVA-ST-vaccinated aged hamsters.

2. Materials and Methods

Ethics statement. Male Syrian hamsters (66 week-old, Mesocricetus auratus; breed RjHan:AURA) were bought from the Janvier Labs (SAINT BERTHEVIN CEDEX, France). We housed the hamsters under specified pathogen-free conditions, with free access to water and food. Before the immunization with non-recombinant MVA-vaccine or MVA-ST vaccine, the hamsters adapted to our stables for at least one week. Our hamster studies fully meet the requirements of the European and national regulations for animal experimentation (European Directive 2010/63/EU; Animal Welfare Acts in Germany) and Animal Welfare Act, approved by the Niedersächsisches Landesamt für Verbraucherschutz und Lebensmittelsicherheit (LAVES) Lower Saxony, Germany). After SARS-CoV-2 challenge, the animals were housed in individually ventilated cages (IVCs; Tecniplast, Buguggiate, Italy) in approved BSL-3 facilities. All animal and laboratory work involving infectious SARS-CoV-2 was done and facilitated in a biosafety level (BSL)-3e laboratory and facilities at the Research Center for Emerging Infections and Zoonoses, University of Veterinary Medicine, Hannover.

Immunization experiments in hamsters. Male Syrian hamsters (66 week-old, Mesocricetus auratus; breed RjHan:AURA) were immunized with 10^8 PFU recombinant MVA-ST or empty-MVA-vector control intramusculary into the quadriceps muscle of the left hind leg. Second immunization (Boost-immunization) was applicated 21 days later. We closely observed and monitored the hamsters after the immunizations for well-being, health constitution and clinical signs as represented in a clinical score. We also monitored the body weights daily. For further analysis, we collected blood at different time points (days 0, 21, 42 and 55) after the immunization. Serum was prepared by centrifugation of the coagulated blood at 1300 × g for 5 min in serum tubes (Sarstedt AG&Co., Germany). Serum samples were then stored at -80 °C until further evaluations.

SARS-CoV-2-infection experiments in Syrian hamsters. We performed challenge-infection by the intranasal route with $1x10^4$ TCID50 of SARS-CoV-2 (Isolate Germany/BavPat1/2020, NR-52370) received from BEI Resources, NIAID, NIH under anesthesia. After respiratory challenge the hamsters were monitored at least twice per day for well-being, health constitution and clinical signs using a clinical score sheet by allocating to one of the following categories of COVID-19 disease specific symptoms: Cardiovascular system, fur/ skin condition, lower respiratory tract, upper respiratory tract, environment social behaviour/ general condition/ locomotion and neurological scoring. Body weights were checked daily.

Virus. SARS-CoV-2 (Isolate Germany/BavPat1/2020) received from BEI Resources, NIAID, NIH was amplified in VeroE6 cells (ATCC #CRL-1586) in DMEM (Sigma-Aldrich GmbH) including 2% fetal bovine serum, 1% penicillin-streptomycin and 1% L-glutamine at 37°C. Experiments including SARS-CoV-2-infection were conducted in biosafety level-3 laboratories at the RIZ, University of Veterinary Medicine Hannover, Germany. The recombinant MVA candidate vaccine expressing a prefusion-stabilized version of SARS-CoV-2 spikeprotein (MVA-ST) was generated as previously described [10]. MVA-ST has been amplified on DF-1 cells and purified by sucrose-gradient as previously described [10].

Plaque reduction neutralization test ($PRNT_{50}$). Plaque reduction neutralization tests ($PRNT_{50}$) were done to evaluate the titers of neutralizing antibodies against SARS-CoV-2 in serum samples. SARS-CoV-2 (Isolate Germany/BavPat1/2020) obtained from BEI Resources, NIAID, NIH was used for the infection of VeroE6 cells in the $PRNT_{50}$ assay. Heat-inactivated serum samples were plated as duplicates in 2-fold dilutions in 50 µl DMEM on 96-well-plates. 50 µl of SARS-CoV-2 (600 $TCID_{50}$) was added per well and incubated at 37°C for 1 h. After incubation the mixtures was placed on VeroE6 cells using 96-well plates and incubated for 45 min. 100 µl DMEM mixed 1:1 with Avicel RC-591 (Dupont, Nutrition & Biosciences) was layered on each well and the plates were incubated for 24 h at 37°C. Finally, the cells were fixed with 4% formaldehyde/PBS for further staining. For this, a

 doi:10.20944/preprints202311.1882.v1

polyclonal rabbit antibody targeting the SARS-CoV-2 nucleoprotein (clone 40588-T62, Sino Biological) was used. A secondary peroxidase-labeled goat anti-rabbit IgG (Dako, Agilent) was used to develop a signal after adding a precipitate forming TMB substrate (True Blue, KPL SeraCare). Counts of infected cells with SARS-CoV-2 was measured with the ImmunoSpot® reader (CTL Europe GmbH). Using the the BioSpot™ Software Suite the serum neutralization titer ($PRNT_{50}$) was calculated. For this, the reciprocal of the highest serum dilution leading to a reduction of >50% of the plaque formation by SARS-CoV-2 infection was used.

Measurement of viral burden. To analyze the viral load in nasal or oropharyngeal swabs, swabs were taken either from the nose or from the oropharynx by rotating the tip of the swabs. After sampling, swabs were then dissociated and lysed in 1ml DMEM containing P/S (penicillin and streptomycin, Gibco). To analyze the viral load in the lungs of infected hamsters, tissue samples were taken after euthanasia and further prepared by homogenization in 1 ml DMEM containing P/S (penicillin and streptomycin, Gibco). Homogenization was performed with the TissueLyser-II (Qiagen) and the homogenate was stored at -80°C until further use. To determine the titers of infectious SARS-CoV-2, lung-homogenates or swab lysates, in DMEM containing 5% FBS, were incubated in serial 10-fold dilutions on Vero cells in 96-well-plates. After four days of incubation at 37°C, the median tissue culture infectious dose ($TCID_{50}$ units / ml) was calculated using the Reed-Muench method based on cytopathic effects in the cells. For statistical analysis, the data points of samples which did not induce cytopathic effects, were changed to half of the detection limit. To determine levels of viral RNA of SARS-CoV-2 in the lungs, RT-qPCR (quantitative real-time reverse transcription PCR) analysis targeting different genes of SARS-CoV-2 were conducted. Using the KingFisher Flex, RNA was extracted from lung tissue samples with the NucleoMag RNA kit according to the manufacturer's protocol. For SARS-CoV-2 RNA amplification, the Luna® Universal Probe One-Step RT-qPCR Kit (NEB #E3006, New England Biolabs GmbH, Frankfurt am Main, Germany) was used in a CFX96-Touch Real-Time PCR system (Bio-Rad). The RT-qPCR assay specific for the RdRp gene of SARS-CoV-2 and recommended by the WHO, were used: SARS-2-IP4, forward primer (5'- GGT AAC TGG TAT GAT TTC G -3'), reverse primer (5'- CTG GTC AAG GTT AAT ATA GG-3') and probe (5'-TCA TAC AAA CCA CGC CAG G-3' [5']FAM [3']BHQ-1)]. The RT-qPCR assay specific for the subgenomic E of SARS-CoV-2 used the following primers: forward primer (5' ATATTGCAGCAGTACGCACACA -3'), reverse primer (5' CGATCTCTTGTAGATCTGTTCTC -3') and probe (5' ACACTAGCCATCCTTACTGCGCTTCG -3' [5']FAM [3']BBQ]. The RT-qPCR assay specific for the E gene of SARS-CoV-2 used the following primers: forward primer (5' ACAGGTACGTTAATAGTTAATAGCGT-3'), reverse primer (5' ATATTGCAGCAGTACGCACACA-3') and probe (5' ACACTAGCCATCCTTACTGCGCTTCG-3' [5']FAM [3']BBQ]. The PCR program included reverse transcription at 50˚C for 10 min; denaturation at 95˚C for 1 min; 44 cycles of 95˚C for 10 sec (denaturation), and 56˚C for 30 sec (annealing and elongation). The relative fluorescence units (RFU) were measured at the end of the elongation step. The sample Ct value was correlated to a standard RNA transcript and the quantity of viral RdRp copy numbers per µl of total RNA was calculated.

Histological evaluation of lung pathology in hamsters. Injection and plunging of 10% buffered formalin in the lung was done for fixation purposes. Left lung lobe tissue samples were further embedded in paraffin and 2-3 µm thick sections were generated. Hematoxylin and eosin (HE) staining was performed for the evaluation of lesions in the lung. Analysis was done blinded with a semi-quantitative scoring system. Briefly, the evaluation included assessment of alveolar lesions (inflammation, regeneration, necrosis/desquamation and loss of alveolar cells, atypical large/syncytial cells, intraalveolar fibrin, alveolar edema, hemorrhage), airway lesions (inflammation, necrosis, hyperplasia) and vascular lesions (vasculitis, perivascular cuffing, edema, and hemorrhage). The total scores reflect the sum of all scores in the respective lung anatomical compartments. Details on the scoring system have been described previously [11].

Immunohistochemistry targeting the Nucleocapsid of SARS-CoV-2. Formalin-fixed, paraffin-embedded lung tissue samples were stained using a monoclonal mouse antibody (Sino Biological,

 doi:10.20944/preprints202311.1882.v1

40143-MM0) against the nucleoprotein of SARS-CoV-2 and the Dako EnVision+ polymer system (Dako Agilent Pathology Solutions) as described previously [12].

To quantify SARS-CoV-2 NP immunolabeled cells in pulmonary tissue, slides were digitized using a slide scanner (Olympus VS200 Digital; Olympus Deutschland GmbH). QuPath (version 0.3.1) was used to perform Image analysis [13]. Detection of lung tissue was performed automatically using digital thresholding. Images of whole slides of the entire left lung were evaluated. Blood vessels as well as artifacts were subtracted from the total lung tissue as they were indicated as ROIs. Automated positive cell detection was used, as previously described [14], to quantify the immune-stained cells in the lung tissue. This was based on marker-specific thresholding parameters.

Enzyme-linked Immunospot (ELISpot). Hamsters were euthanized on day 6 after challenge infection and splenocytes were isolated immediately. For this, spleens were smashed on a 70-µm strainer (Falcon®, Sigma-Aldrich, Taufkirchen, Germany) and flushed and solved with RPMI-10 (RPMI 1640 medium containing 10% FBS, 1% Penicillin-Streptomycin, 1% HEPES; Sigma-Aldrich, Taufkirchen, Germany). Lysis of red blood cells were conducted with Red Blood Cell Lysis Buffer (Sigma-Aldrich, Taufkirchen, Germany). After one washing step, cells were resuspended in RPMI-10. $2x10^5$ splenocytes were counted with the MACSQuant (Miltenyi Biotec B.V. & Co. KG, Bergisch Gladbach, Germany) and seeded per well in 96 well round bottom plates (Sarstedt, Nümbrecht, Germany). For stimulation, three different peptide pools of overlapping peptides obtained by JPT Peptide Technologies (Berlin, Germany) were used. Each peptide consists of 15 amino acids (15mers) overlapping in 11 amino acids. Two of the peptide pools consisted of 157 and 158 overlapping peptides (1µg peptide/mL RPMI 1640) comprising the whole spike glycoprotein of SARS-CoV-2. One additional peptide pool was used for stimulation, which consists of 59 overlapping peptides (1 µg peptide/mL RPMI 1640) comprising the whole nucleocapsid protein of SARS-CoV-2 (BEI Resources, NIAID, NIH). This antigen is not present in the evaluated vaccine. Positive and negative controls were created by stimulation of the cells with phorbol myristate acetate and ionomycin (PMA, SIGMA-ALDRICH, Taufkirchen, Germany) as well as the use of non-stimulated cells. Plates with PVDF membranes (Mabtech, Nacka, Sweden) were coated with a hamster specific anti- IFN-γ monoclonal antibody (Mabtech, Nacka, Sweden). Cells were then placed on the coated plates and incubated for 36 h at 37°C. The inoculum was removed and biotinylated anti-IFN-γ monoclonal antibody was added. After incubation, streptavidin ALP followed by BCIP/NBT-plus substrate was added. Washing steps were done in between all steps as well. The generated spots were scanned and counted with the automated ELISpot Reader ImmunoSpot S6 ULTIMATE UV Image Analyzer (Immunospot, Bonn, Germany) and further analyzed with the ImmunoSpot 7.0.20.1 software.

Flow cytometry. For phenotype characterization, cells were isolated from lungs via digestion using RPMI 1640 supplemented with 10% FCS, 1 mg/ml Collagenase (GENAXXON bioscience GmbH, Ulm) and 0,5 mg/ml DNase (Roche, Merck KGaA, Darmstadt) for 30 minutes at 37 °C. Subsequently, digested lungs were smashed with scissors and flushed with RPMI-10 (RPMI 1640 medium containing 10% FBS, 1% Penicillin-Streptomycin; Sigma-Aldrich, Taufkirchen, Germany) through a 70-µm strainer (Falcon®, Sigma-Aldrich, Taufkirchen, Germany). Incubation with Red Blood Cell Lysis Buffer (Sigma-Aldrich, Taufkirchen, Germany) lysed red blood cells. After a washing step, cells were resuspended in RPMI-10 medium. The cells were counted with the MACSQuant (Miltenyi Biotec B.V. & Co. KG, Bergisch Gladbach, Germany) and dead cells were visualized by staining $4x10^5$ lung cells with LIVE/DEAD fixable Near IR stain kit (InvitrogenTM, Thermo Fisher Scientific, Waltham, USA) according to the manufacturer's instructions followed by fixation using 4% formaldehyde/PBS for 20 minutes. $2x10^5$ cells were stained with antibodies against CXCR3 (RRID: AB_2743928), CD4 (RRID: AB_464894) and CD3 (RRID:AB_10841760) in a total volume of 200 µl for 30 minutes. After washing, cells were measured using the MACSQuant (Miltenyi Biotec B.V. & Co. KG, Bergisch Gladbach, Germany).

Analysis of IL-7 by Real-time-PCR. Extracted RNA from lung tissue samples was amplified in a CFX96-Touch Real-Time PCR system (Bio-Rad) using the commercially available Luna® Universal One-Step RT-qPCR Kit (NEB #E3005, New England Biolabs GmbH, Frankfurt am Main, Germany). The RT-qPCR assay specific for the hamster IL-7 used the following primers: forward primer (5'-

 doi:10.20944/preprints202311.1882.v1

ATCCAAGCCACAAAAATAAAGCC-3′) and reverse primer (5′-TTTCTTGCTGTCACTGCTTTG-3′). To normalize values, ß-Actin was used as housekeeping gene using (5′-CCAAGGCCAACCGTGAAAAG-3′) as forward primer and (5′-ATGGCTACGTACATGGCTGG-3′) as reverse primer.

The PCR program included reverse transcription at 55˚C for 10 min; denaturation at 95˚C for 1 min; 44 cycles of 95˚C for 20 sec (denaturation), and 56˚C for 30 sec (annealing and elongation). The relative fluorescence units (RFU) were measured at the end of the elongation step. Amount of IL-7 relative to the housekeeping gene was calculated using the Ct method.

Statistical analysis. Data were prepared using GraphPad Prism 9.0.0 (GraphPad Software Inc., San Diego CA, USA). Data sets were analyzed for normal distribution using D'Agostino & Person test or Shapiro-Wilk-test. Normally distributed data were analyzed for differences using t-test or 2-way-ANOVA and expressed with mean. Not-normally distributed data were analyzed for differences using Mann-Whitney-test and Friedman test and expressed as median. A P value < 0.05 indicates the threshold for statistical significance.

3. Results

3.1. MVA-ST vaccination induced protection after SARS-CoV-2 challenge in aged Syrian hamsters

Syrian hamsters aged 66 weeks were vaccinated with 10^8 PFU of empty MVA-vector control or MVA-SARS-2-ST (MVA-ST) via the intramuscular route. 21 days later all hamster were boosted (Figure 1A). Safety and immunogenicity were analyzed as established before [10]. No clinical disease outcome or weight loss could be detected in MVA-control or aged hamsters immunized with MVA-ST (Suppl. Figure 1). No SARS-CoV-2 neutralizing antibodies were determined in sera from aged hamsters that received empty MVA-vector control vaccine (<1:20, Figure 1B). In contrast, all MVA-ST vaccinated animals produced easily detectable neutralizing antibodies with an average $PRNT_{50}$ titer of 1:350 already at 3 weeks after priming (Figure 1B). After the boost vaccination on day 21, we measured higher amounts of SARS-CoV-2 neutralizing antibodies in all sera from aged hamsters vaccinated with MVA-ST with an average titer of 1:600 $PRNT_{50}$ (Figure 1B).

After intranasal SARS-CoV-2 infection, all hamsters lost about 5% body weight 2 days post infection (dpi). MVA-vaccinated control hamsters continued to show progressive weight loss until 6 dpi, losing approximately 15% of the original body weight as measured on the day of challenge. In contrast, no further loss of body weight was identified for MVA-ST vaccinated hamsters (Figure 1C). Control animals developed significant clinical symptoms with enhanced breathing, scruffy fur and reduced activity culminating until day 6 with a total score of 6. Minimal COVID-19-specific symptoms were observed in MVA-ST-vaccinated animals with a cumulative score ranging between 0.5-1 on days 4-6 (Figure 1D) mainly resulting in ruffled fur without any respiratory symptoms. Three dpi, significant levels of infectious SARS-CoV-2 were detected in oropharyngeal and nasal swabs of control hamsters (median $6.3x10^3$ $TCID_{50}$ in oropharyngeal, median $1.99x10^3$ in nasal swabs; Figure 2A and B). MVA-ST-vaccinated animals had significantly reduced titers of infectious SARS-CoV-2 in oropharyngeal swabs (median $2x10^2$ $TCID_{50}$; Figure 2A) and nasal swabs (median $4.7x10^1$ $TCID_{50}$; Figure 2B).

Preprints (www.preprints.org) | NOT PEER-REVIEWED | Posted: 29 November 2023 doi:10.20944/preprints202311.1882.v1

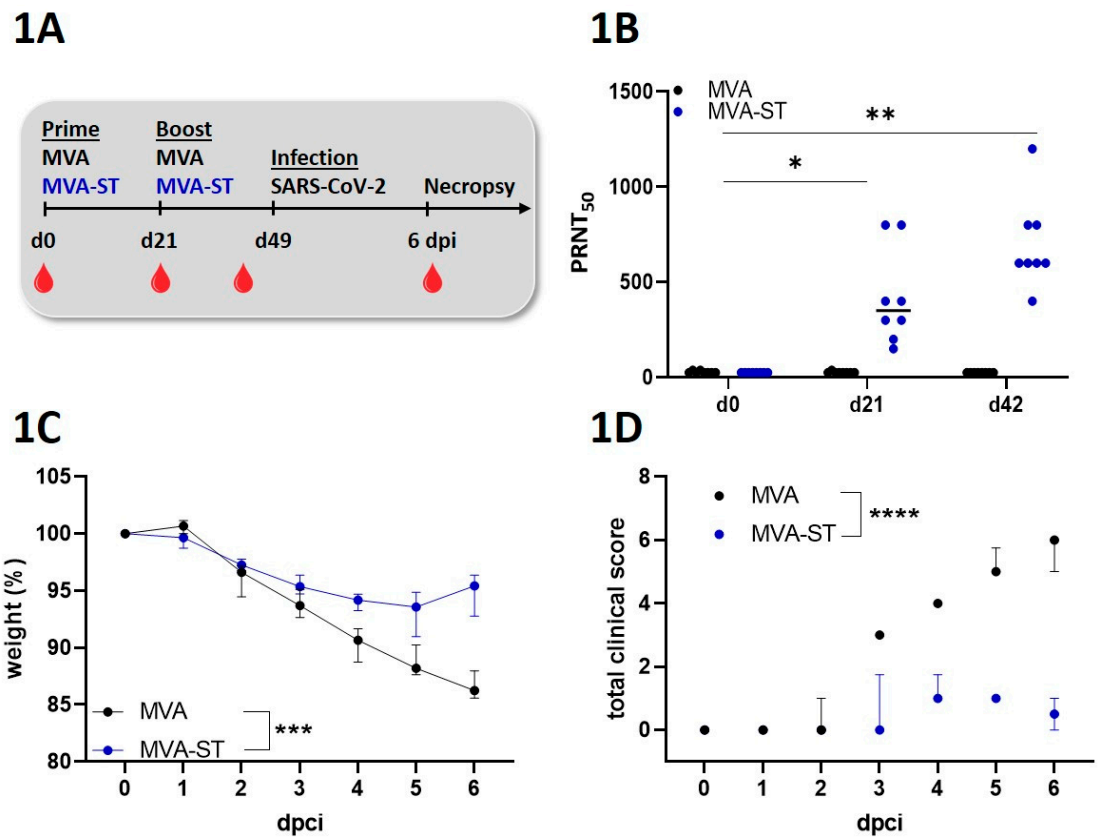

Figure 1. Immunogenicity and efficacy of MVA-ST-immunization in aged hamsters. (A) Animals were vaccinated by intramuscular route twice with 10^8 PFU MVA-ST (n=7) over a 21-day interval. Blood samples were taken at day 0, at day 21 post 1st immunization (prime) or at day 42 post 1st immunization (day 21 post 2nd immunization) and 6 days post challenge. Hamsters vaccinated with empty MVA-vector (MVA, n=7) served as controls. Body weight changes, clinical scores, viral loads, pathology and immunogenicity were determined. (B) Sera were analyzed for SARS-CoV-2 neutralizing antibodies using plaque reduction assay ($PRNT_{50}$) on day 0, 21 and 42 after initial vaccination. (C) After challenge infection on day 49, changes in body weights were monitored daily, (D) a clinical score sheet was used to monitor spontaneous behavior, clinical disease and general condition. Differences between groups were analyzed by Dunn's multiple comparisons test of AUC. Asterisks represent statistically significant differences between two groups: * $p < 0.05$, ** $p < 0.01$, *** $p < 0.001$, **** $p < 0.0001$.

All animals were euthanized 6 dpi, and blood samples, lungs and spleens were taken for further analysis. In the lungs, we detected substantial titers of infectious SARS-CoV-2 of control hamsters (median $3.9x10^3$ $TCID_{50}$) but no titers of SARS-CoV-2 were measured in the lungs of MVA-ST immunized hamsters (Figure 2C), as further confirmed by qRT-PCR analysis (Figure 2D-F).

Preprints (www.preprints.org) | NOT PEER-REVIEWED | Posted: 29 November 2023 doi:10.20944/preprints202311.1882.v1

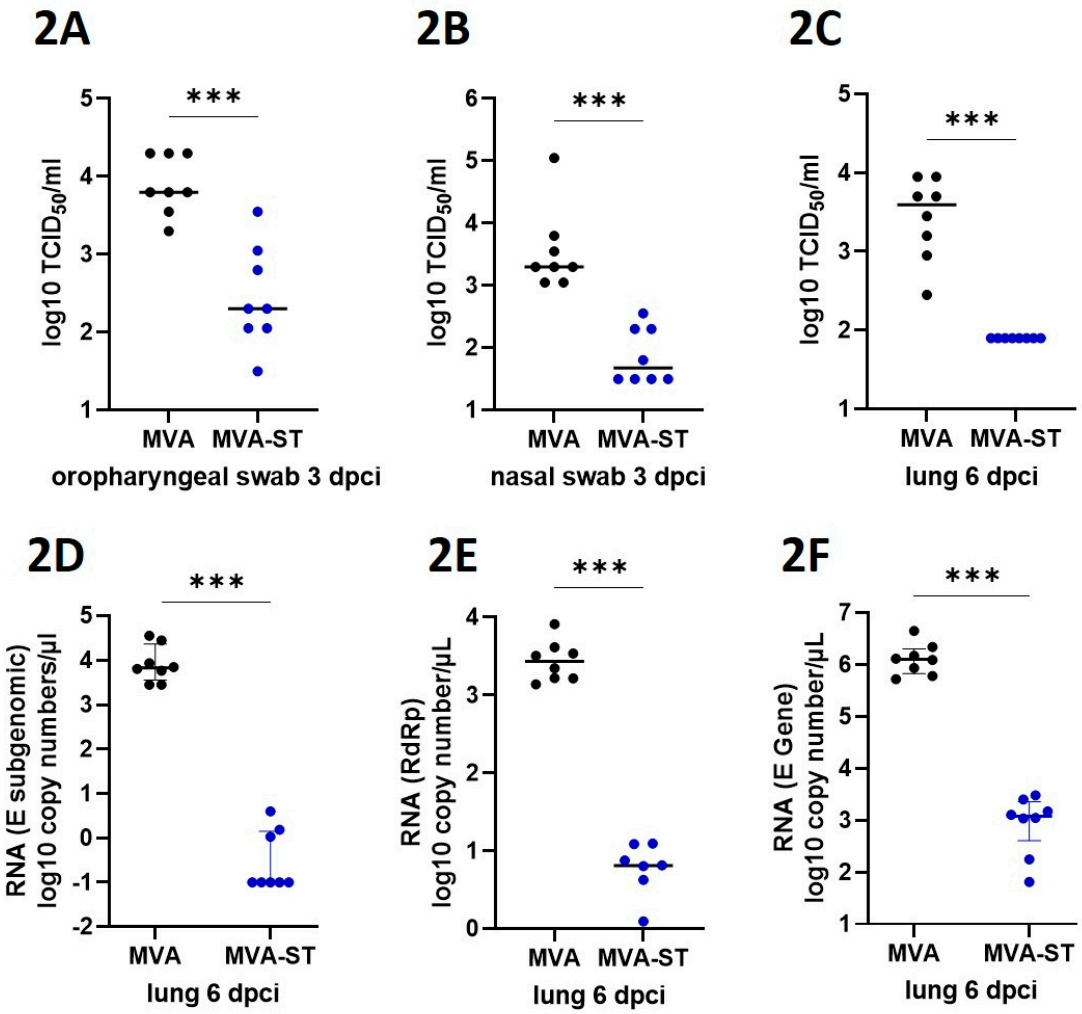

Figure 2. Reduction of viral burden in the lungs induced after MVA-ST immunization in aged Syrian hamsters. MVA-ST-aged hamsters (n=7) and MVA-control-aged hamsters (=7) were challenged with 10^4 $TCID_{50}$ SARS-CoV-2 Bav Pat1 isolate via the intranasal route. Body weight changes, clinical scores, viral loads, pathology and immunogenicity were determined. (A) Oropharyngeal and (B) nasal swabs were taken on day 3 after challenge infection and evaluated for the titers of SARS-CoV-2 by $TCID_{50}$. (C) At the day of death, lungs were prepared and evaluated for the amounts of infectious SARS-CoV-2 using $TCID_{50}$/gram lung tissue and (D-F) using different PCR-assays for SARS-CoV-2 gRNA copies. Differences between groups were analyzed by Dunn's multiple comparisons test. Asterisks represent statistically significant differences between two groups: * $p < 0.05$, ** $p < 0.01$.

Pathohistological analysis of hematoxylin and eosin-stained lung sections revealed large areas of lung consolidation and inflammation in control hamsters (Figure 3A). In the alveolar lesions, accumulation of neutrophils and mononuclear cells were detected that enlarged also to alveolar septae and filled alveolar lumina. These pathological changes were significantly reduced or nearly absent in MVA-ST-vaccinated animals (Figure 3B). Immune staining specific for the nucleoprotein of SARS-CoV-2 showed high amounts of nucleoprotein positive cells in the lungs of control vaccinated animals (MVA) in contrast to significantly lower amounts of positive cells in hamsters vaccinated with MVA-ST (Figure 3C).

Preprints (www.preprints.org) | NOT PEER-REVIEWED | Posted: 29 November 2023 doi:10.20944/preprints202311.1882.v1

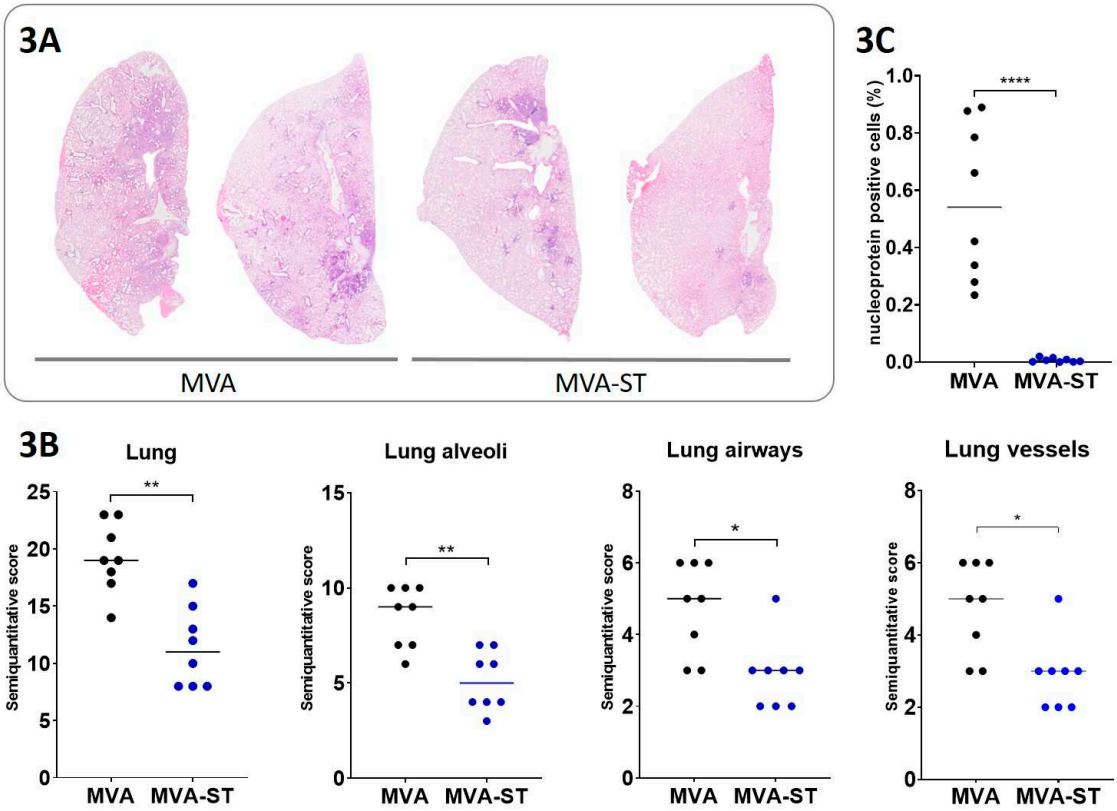

Figure 3. MVA-ST induced lung protection. (A) Representative overview images of hematoxylin and esosin-stained lung sections. (B) Lung lesions were graded using semiquantitative scoring systems for histopathological lesions in lungs. (C) Nucleoprotein positive cells were detected by Immuno-Histo-Staining. Differences between groups analyzed by t-Test. Asterisks represent statistically significant differences between two groups: *p < 0.05, **p < 0.01, ***p < 0.001, ****p < 0.0001. .

3.2. MVA-ST induced immune responses correlate with protection against SARS-CoV-2 infection in aged Syrian hamsters

After challenge infection, we detected levels of virus neutralizing antibodies even in sera of control-vaccinated hamsters (mean 1:4200 $PRNT_{50}$). In MVA-ST vaccinated hamsters, the titers significantly increased to average $PRNT_{50}$ titers of 1:8400 $PRNT_{50}$ (Figure 4A).

To evaluate the activation of SARS-CoV-2-specific T cells, we prepared splenocytes and lung cells. Splenocytes were restimulated with pools of overlapping peptides comprising either the S1 or S2 subunit of the SARS-CoV-2 S-protein or SARS-CoV-2 N-protein (Suppl. Figure 2) and analyzed using ELISPOT assays. MVA-ST vaccination activated robust numbers of S1-specific T cells with mean numbers of 1011 IFN-γ spot forming cells (SFC) in 10^6 splenocytes (Figure 4B), whereas significantly lower numbers of these cells were detected in control hamsters (mean 163 IFN-γ SFC; Figure 4B). MVA-ST-vaccinated hamsters also mounted substantial levels of S2-specific T cells (mean 2048 IFN-γ SFC), while these cells were again significantly lower in control animals (mean 1371 IFN-γ SFC). Comparable levels of T cells specific for the SARS-CoV-2-N were detected in both groups (MVA: mean 157, and MVA-ST: mean 332 IFN-γ SFC; Figure 4B).

Preprints (www.preprints.org) | NOT PEER-REVIEWED | Posted: 29 November 2023 doi:10.20944/preprints202311.1882.v1

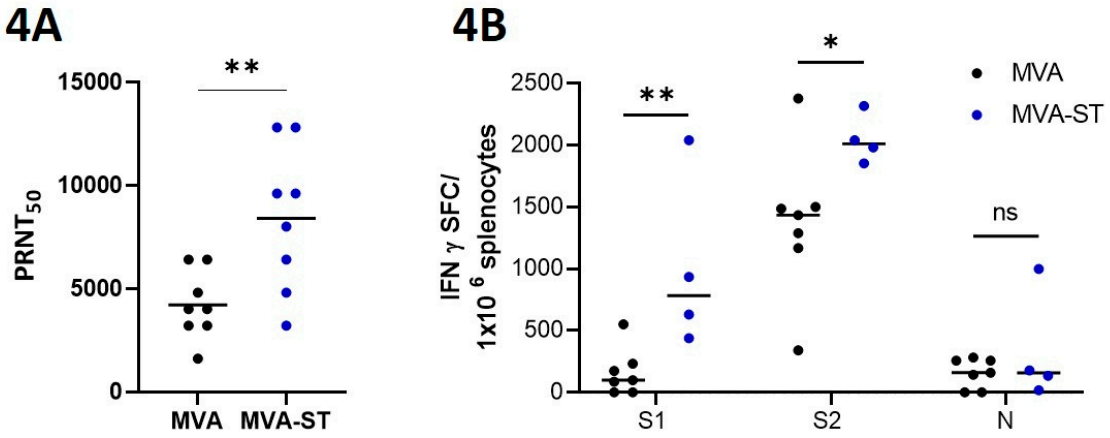

Figure 4. Immune responses after MVA-ST vaccination in serum and spleen. 6 days after the intranasal SARS-CoV-2 infection, sera and splenocytes were produced and evaluated for (A) SARS-CoV-2 neutralization titers measured by plaque reduction assay ($PRNT_{50}$) and (B) SARS-CoV-2 specific T cells in ELISPOT assays. Differences between groups were analyzed by Mann-Whitney test. Asterisks represent statistically significant differences between two groups: * $p < 0.05$, ** $p < 0.01$, *** $p < 0.001$, **** $p < 0.0001$.

We used a panel of hamster reactive antibodies against specific markers (CD3, CD4, CXCR3 [15]) to characterize T cells in the lungs by FACS analysis. MVA-ST-vaccinated hamsters mounted significantly increased levels of T cells defined as CD3+ cells compared to control animals (median 34% vs. 26%; Figure 5A). Similarly, significantly higher levels of CD4+ T cells were present in MVA-ST-vaccinated animals than in control animals (median 31% vs. 25%; Figure 5B). CXCR3+ CD4+ T cells were also significantly increased in MVA-ST-vaccinated hamsters (median 0,26 %) compared to control hamsters (median 0.035%; Figure 5C). We also measured increased levels of IL-7 in lungs from MVA-ST-vaccinated animals (median 4.45x10-4; Figure 5E) than control hamsters (median 2.62x10-6). We then analyzed the expression of TCR as measured by CD3 expression on CD4+ T cells; control hamsters mounted significantly higher expression of TCR (median 5,8%; Figure 5D) than MVA-ST-vaccinated animals (median 4.3%; Figure 5D). In summary, MVA-ST vaccination protected aged hamsters from COVID-19 and activated robust levels of SARS-CoV-2 specific immune responses.

Preprints (www.preprints.org) | NOT PEER-REVIEWED | Posted: 29 November 2023 doi:10.20944/preprints202311.1882.v1

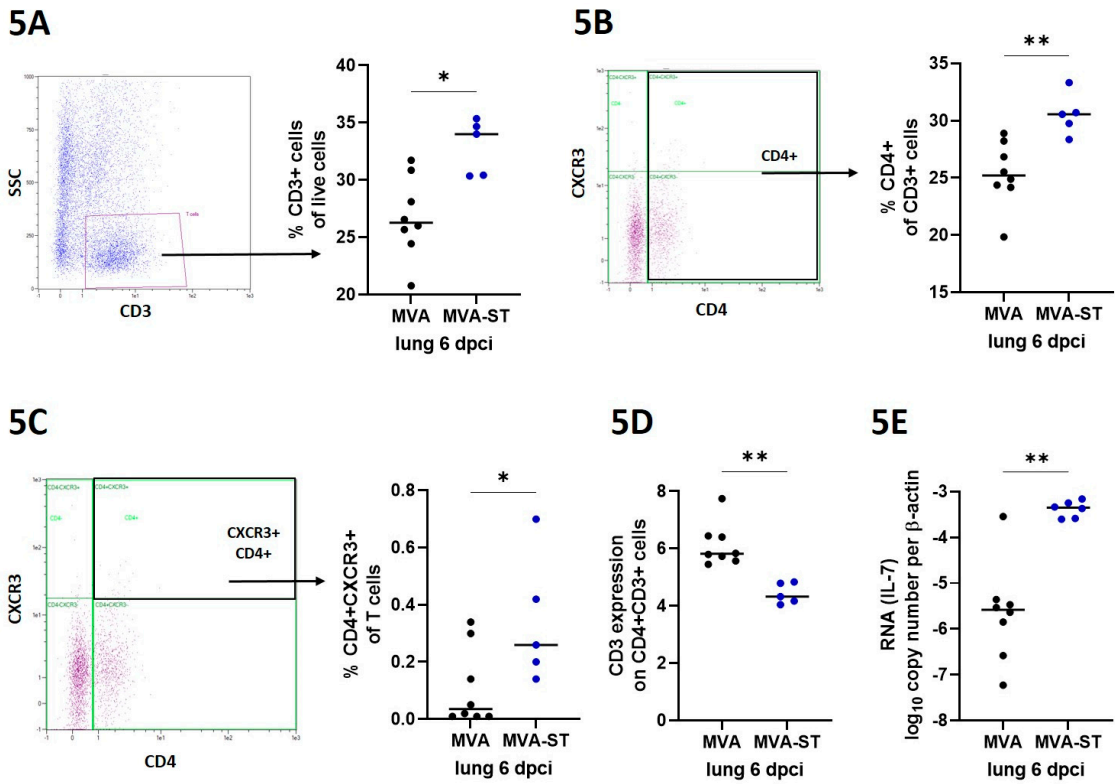

Figure 5. Immune responses after MVA-ST vaccination in the lung. 6 days after SARS-CoV-2 infection, lung cells were prepared and evaluated in flow cytometry for (A) CD3-, (B) CD4- and (C) CXCR3-specific antibodies. (D) CD3 expression on CD3+CD4+-positive lung cells and (E) levels of IL-7 in lungs measured by qRT-PCR. Differences between groups analyzed by t-Test, Mann-Whitney test or 2way ANOVA. Asterisks represent statistically significant differences between two groups: *p < 0.05, **p < 0.01, ***p < 0.001.

4. Discussion

Immunosenescence is a known problem for successful vaccination in elderly people [16]. In this study, we used 66-week-old hamsters, which correlates to about 65 years in human age [17]. In agreement with data from previous studies evaluating the effects of COVID-19 vaccinations in different human age groups [18], we observed altered protection in aged MVA-ST-vaccinated hamsters compared to the equivalent adult hamster model [10]. Our results demonstrated that the immunogenicity and protective outcome of MVAT-ST-immunization in the old hamsters was different from the MVA-ST immunization in normal aged hamsters. Here, we confirmed significant immunogenicity and efficacy of MVA-ST-prime-boost immunizations [10]. In the aged hamsters, following infection-challenge after MVA-ST vaccination, we detected minimal disease outcome, with marginal body weight loss, clinical symptoms and viral shedding from the upper respiratory tract. This is in line with data from humans when break-through infections with mild clinical disease have been confirmed in vaccinated people with a mean age of 71.1 [19,20]. An effect of immunosenescence is also seen for the control-aged hamsters, where we observed more severe SARS-CoV-2 disease outcomes compared to adult hamsters [10]. We also detected more severe lung pathology with massive extents of alveolar inflammation and damage, confirming other studies characterizing SARS-CoV-2 pathogenesis in aged hamsters [4–6]. Similarly, in elderly people, SARS-CoV-2 infection often results in severe disease with more pronounced lung pathology. In addition to minimal clinical symptoms and reduced viral shedding from the upper respiratory tract, we detected no viral load and significantly reduced levels of lung damage in aged MVA-ST-vaccinated hamsters, indicating a robust protective capacity.

MVA is an attenuated, replication deficient candidate vaccine with a well-established safety profile and excellent immunostimulatory effects. This is already confirmed as a smallpox vaccine where MVA has been successfully administered to persons at risk, e.g. with atopic dermatitis or infected with HIV [21–23]. Thus, MVA seems excellently suited to overcome the limitations of vaccination in the elderly. This has already been successfully confirmed for an MVA-based vaccine against influenza in a clinical phase I study [24].

In line with clinical data from Flu vaccine development, we confirmed the suitability of our MVA-ST vaccine in hamsters as a surrogate model for COVID-19 in humans. This was emphasized by the strong activation of neutralizing antibodies in MVA-ST-vaccinated animals even before challenge infection. After SARS-CoV-2 challenge, we also detected SARS-CoV-2-neutralizing antibodies in control animals despite the absence of obvious protective efficacy, possibly resulting from fulminant viral infection in the upper respiratory tract. Another hypothesis is that these increased titers of SARS-CoV-2-specific antibodies are involved for the outcome of severe COVID-19 disease. This has been demonstrated in elderly people with more severe disease who exhibited higher antibody reactivity [25]. In this context, cellular immunity correlated with more robust and solid protection independent of humoral immunity [26].

Notably, compared to the control hamsters, we demonstrate that MVA-ST-vaccinated elderly hamsters mount robust activation of T cells. Especially within the lung, the main target organ for COVID-19, we detected significantly increased titers of activated CD4+ T cells, as seen for CXCR3+ cells. Such strong immunostimulation is a well-known characteristic of MVA-based vaccines and mainly correlates with a potent activation of innate immune signaling leading to chemokine and cytokine induction, generating an optimal immunological milieu for antigen-specific immunity [27]. To support this, MVA-ST-vaccinated hamsters mounted significantly increased levels of IL-7. Diminished activation of proinflammatory cytokines including IL-7 has been confirmed to be involved in the outcome of immunosenescence [28]. Advanced activation of the innate immunity might explain the improved activation of antigen-specific T cells in MVA-ST-vaccinated animals. This is further confirmed not only by increased levels of CD4+ T cells lacking TCR on the surface, indicating activation of antigen-specific T cells [29], but also when we detected significantly increased levels of S1- and S2-specific T cells in the spleens of MVA-ST-vaccinated hamsters. Future studies will be of interest to characterize the role of these SARS-CoV-2 S-specific T cells in more detail concerning the outcome of infection and/or vaccine induced protection.

In summary, our aged-hamster model confirmed the robust activation of SARS-CoV-2-specific immunity after MVA-ST-immunization, likely involved in protection against severe clinical disease outcome.

5. Conclusions

In conclusion, our findings further indicate that the success of MVA-ST vaccination is not hampered by age-related changes in the immune system. Our results further support MVA vector vaccine-induced safety, immunogenicity and efficacy in elderly individuals as an important aspect of population-based immunity against COVID-19, and likely also against other betacoronavirus specific diseases such as the Middle East Respiratory syndrome. We therefore highlight a promising approach for developing MVA-based vaccination for elderly people that result in more robust activation of antigen-specific T cells as a strategy to overcome immunosenescence, also for other pathogens.

Supplementary Materials: The following supporting information can be downloaded at the website of this paper posted on Preprints.org. Figure S1-S2: MVA-ST vaccination in aged hamsters

Author Contributions: Conceptualization, A.V., S.C.; methodology, A.V., S.C., L.M.S., F.A.; formal analysis, A.V., S.C., L.M.S., F.A., C.M.z.N., T.T., A.T., M.C., W.B., G.S.; investigation, A.V., S.C., L.M.S., F.A., C.M.z.N., T.T., A.T., M.C.; writing—original draft preparation, A.V., S.C., L.M.S.; writing—review and editing, A.V., S.C., L.M.S., L.M.S., F.A.; project administration, A.V., funding acquisition, A.V. All authors have read and agreed to the published version of the manuscript.

Funding: This work was supported by Federal Ministry of Education and Research (BMBF RAPID 01KI1723G and ZOOVAC 01KI1718 to AV).

Data Availability Statement: The datasets generated during and/or analyzed during the current study are available from the corresponding authors upon reasonable request.

Acknowledgments: We thank Monika Berg, Saskia Oppermann, Darren Markillie, Matthias Herberg, Bernd Vollbrecht, and Sandra Pfeifer for expert help in animal studies.

Conflicts of Interest: All authors: No reported personal conflicts of interest. All authors attest they meet the ICMJE criteria for authorship.

References

1. Dorjee, K., et al., *Prevalence and predictors of death and severe disease in patients hospitalized due to COVID-19: A comprehensive systematic review and meta-analysis of 77 studies and 38,000 patients.* PLoS One, 2020. **15**(12): p. e0243191.
2. Bates, T.A., et al., *BNT162b2-induced neutralizing and non-neutralizing antibody functions against SARS-CoV-2 diminish with age.* Cell Rep, 2022. **41**(4): p. 111544.
3. Lu, Y., et al., *Effect of Age on Relative Effectiveness of High-Dose Versus Standard-Dose Influenza Vaccines Among US Medicare Beneficiaries Aged ≥65 Years.* J Infect Dis, 2019. **220**(9): p. 1511-1520.
4. Oishi, K., et al., *A diminished immune response underlies age-related SARS-CoV-2 pathologies.* Cell Rep, 2022. **39**(13): p. 111002.
5. Osterrieder, N., et al., *Age-Dependent Progression of SARS-CoV-2 Infection in Syrian Hamsters.* Viruses, 2020. **12**(7).
6. Imai, M., et al., *Syrian hamsters as a small animal model for SARS-CoV-2 infection and countermeasure development.* Proc Natl Acad Sci U S A, 2020. **117**(28): p. 16587-16595.
7. McLean, C., et al., *Persistence of immunological memory as a potential correlate of long-term, vaccine-induced protection against Ebola virus disease in humans.* Front Immunol, 2023. **14**: p. 1215302.
8. Agency, E.M. *Medicines - Mvabea*. 2023 14.08.2023 04.10.2023]; Available from: https://www.ema.europa.eu/en/medicines/human/EPAR/mvabea.
9. Bockstal, V., et al., *First-in-human study to evaluate safety, tolerability, and immunogenicity of heterologous regimens using the multivalent filovirus vaccines Ad26.Filo and MVA-BN-Filo administered in different sequences and schedules: A randomized, controlled study.* PLoS One, 2022. **17**(10): p. e0274906.
10. Meyer Zu Natrup, C., et al., *Stabilized recombinant SARS-CoV-2 spike antigen enhances vaccine immunogenicity and protective capacity.* J Clin Invest, 2022. **132**(24).
11. Armando, F., et al., *SARS-CoV-2 Omicron variant causes mild pathology in the upper and lower respiratory tract of hamsters.* Nat Commun, 2022. **13**(1): p. 3519.
12. Bošnjak, B., et al., *Intranasal Delivery of MVA Vector Vaccine Induces Effective Pulmonary Immunity Against SARS-CoV-2 in Rodents.* Front Immunol, 2021. **12**: p. 772240.
13. Bankhead, P., et al., *QuPath: Open source software for digital pathology image analysis.* Sci Rep, 2017. **7**(1): p. 16878.
14. Heydemann, L., et al., *Hamster model for post-COVID-19 alveolar regeneration offers an opportunity to understand post-acute sequelae of SARS-CoV-2.* Nat Commun, 2023. **14**(1): p. 3267.
15. Horiuchi, S., et al., *Immune memory from SARS-CoV-2 infection in hamsters provides variant-independent protection but still allows virus transmission.* Sci Immunol, 2021. **6**(66): p. eabm3131.
16. Ciabattini, A., et al., *Vaccination in the elderly: The challenge of immune changes with aging.* Semin Immunol, 2018. **40**: p. 83-94.
17. S. Dutta, P.S., *Age of Laboratory Hamster and Human: Drawing the Connexion.* Biomedical & Pharmacology Journal, 2019. **12**(1): p. p. 49-56.
18. Collier, D.A., et al., *Age-related immune response heterogeneity to SARS-CoV-2 vaccine BNT162b2.* Nature, 2021. **596**(7872): p. 417-422.
19. Brosh-Nissimov, T., et al., *BNT162b2 vaccine breakthrough: clinical characteristics of 152 fully vaccinated hospitalized COVID-19 patients in Israel.* Clin Microbiol Infect, 2021. **27**(11): p. 1652-1657.
20. Soiza, R.L., C. Scicluna, and E.C. Thomson, *Efficacy and safety of COVID-19 vaccines in older people.* Age Ageing, 2021. **50**(2): p. 279-283.

21. von Sonnenburg, F., et al., *Safety and immunogenicity of modified vaccinia Ankara as a smallpox vaccine in people with atopic dermatitis.* Vaccine, 2014. **32**(43): p. 5696-702.
22. Greenberg, R.N., et al., *Safety, immunogenicity, and surrogate markers of clinical efficacy for modified vaccinia Ankara as a smallpox vaccine in HIV-infected subjects.* J Infect Dis, 2013. **207**(5): p. 749-58.
23. Colby, D.J., et al., *Safety and immunogenicity of Ad26 and MVA vaccines in acutely treated HIV and effect on viral rebound after antiretroviral therapy interruption.* Nat Med, 2020. **26**(4): p. 498-501.
24. Antrobus, R.D., et al., *A T cell-inducing influenza vaccine for the elderly: safety and immunogenicity of MVA-NP+M1 in adults aged over 50 years.* PLoS One, 2012. **7**(10): p. e48322.
25. Sasson, J.M., et al., *Diverse Humoral Immune Responses in Younger and Older Adult COVID-19 Patients.* mBio, 2021. **12**(3): p. e0122921.
26. Jäger, M., et al., *Immune Responses Against SARS-CoV-2 WT and Delta Variant in Elderly BNT162b2 Vaccinees.* Front Immunol, 2022. **13**: p. 868361.
27. Lehmann, M.H., et al., *Modified vaccinia virus ankara triggers chemotaxis of monocytes and early respiratory immigration of leukocytes by induction of CCL2 expression.* J Virol, 2009. **83**(6): p. 2540-52.
28. Chung, L., et al., *Interleukin 17 and senescent cells regulate the foreign body response to synthetic material implants in mice and humans.* Sci Transl Med, 2020. **12**(539).
29. Mesner, D., et al., *Loss of Nef-mediated CD3 down-regulation in the HIV-1 lineage increases viral infectivity and spread.* Proc Natl Acad Sci U S A, 2020. **117**(13): p. 7382-7391.